Multivariate Regression Analysis for Identifying Key Drivers of Harmful Algal Bloom in Lake Erie

Omer Mermer [1,*], Ibrahim Demir [2,3]

[1] IIHR—Hydroscience and Engineering, University of Iowa, Iowa City, Iowa, USA
[2] River-Coastal Science and Engineering, Tulane University, New Orleans, LA, USA
[3] ByWater Institute, Tulane University, New Orleans, LA, USA

* Corresponding Author: omer-mermer@uiowa.edu

Abstract

Harmful Algal Blooms (HABs), predominantly driven by cyanobacteria, pose significant risks to water quality, public health, and aquatic ecosystems. Lake Erie, particularly its western basin, has been severely impacted by HABs, largely due to nutrient pollution and climatic changes. This study aims to identify key physical, chemical, and biological drivers influencing HABs using a multivariate regression analysis. Water quality data, collected from multiple monitoring stations in Lake Erie from 2013 to 2020, were analyzed to develop predictive models for chlorophyll-a (Chl-a) and total suspended solids (TSS). The correlation analysis revealed that particulate organic nitrogen (PON), turbidity, and particulate organic carbon (POC) were the most influential variables for predicting Chl-a and TSS concentrations. Two regression models were developed, achieving high accuracy with R^2 values of 0.973 for Chl-a and 0.958 for TSS. This study demonstrates the robustness of multivariate regression techniques in identifying significant HAB drivers, providing a framework applicable to other aquatic systems. These findings will contribute to better HAB prediction and management strategies, ultimately helping to protect water resources and public health.

Keywords: Algal bloom, Chlorophyll-a, total suspended solids, multivariate regression, Pearson's correlation coefficient, ANOVA test, relative importance

Highlights:

- Chlorophyll-a and total suspended solids concentrations are predicted using Multivariate regression models with high accuracy.
- Particulate organic nitrogen, turbidity, and particulate organic carbon were identified as the primary drivers influencing harmful algal blooms.
- The ANOVA F-test confirmed the statistical significance of the regression models, validating the influence of key predictors on Chl-a and TSS concentrations.
- The framework provides a scalable approach for predicting HABs in other aquatic systems

Graphical Abstract:

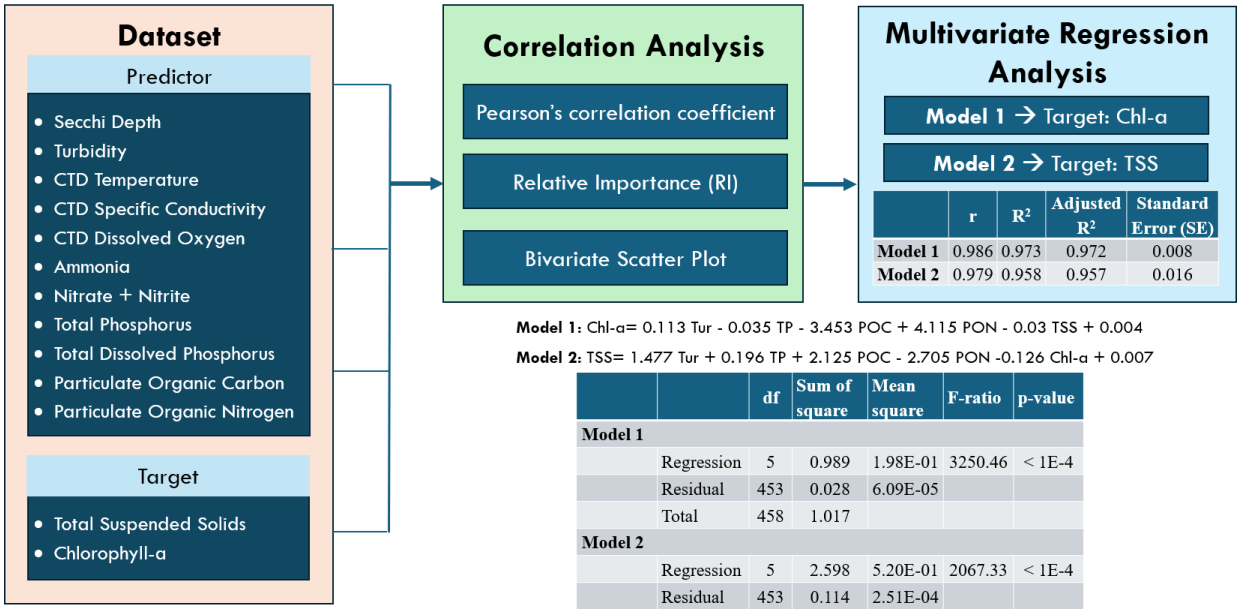

	r	R^2	Adjusted R^2	Standard Error (SE)
Model 1	0.986	0.973	0.972	0.008
Model 2	0.979	0.958	0.957	0.016

Model 1: Chl-a= 0.113 Tur - 0.035 TP - 3.453 POC + 4.115 PON - 0.03 TSS + 0.004

Model 2: TSS= 1.477 Tur + 0.196 TP + 2.125 POC - 2.705 PON -0.126 Chl-a + 0.007

		df	Sum of square	Mean square	F-ratio	p-value
Model 1						
	Regression	5	0.989	1.98E-01	3250.46	< 1E-4
	Residual	453	0.028	6.09E-05		
	Total	458	1.017			
Model 2						
	Regression	5	2.598	5.20E-01	2067.33	< 1E-4
	Residual	453	0.114	2.51E-04		
	Total	458	2.712			

1. Introduction

Environmental contamination has contributed to a significant increase in cyanobacterial biomass (i.e., algae blooms) in water bodies, severely affecting water quality (Baydaroğlu, 2025). The term "bloom" refers to the rapid growth of blue-green algae, or cyanobacteria, which can produce harmful toxins (Carmichael and Falconer, 1993). The emergence and proliferation of Harmful Algal Blooms (HABs), primarily driven by cyanobacteria, has become a critical environmental concern worldwide. These blooms degrade water quality, threaten public health, and disrupt aquatic ecosystems. Key factors fueling the rise in HAB incidents include nutrient pollution, particularly from agricultural runoff and industrial waste (Bayar et al., 2009), as well as climatic changes, such as rising water temperatures and shifts in water quality (Paerl and Paul, 2012; Graham et al., 2016). HABs are known for producing hazardous toxins, undermining the recreational and aesthetic value of waterways, and complicating efforts to provide clean drinking water (Weirich and Miller, 2014). The recent surge in HAB occurrences has been linked to population growth, intensified agricultural practices (Yeşilköy and Demir, 2024; Islam et al., 2024), increasing pollution levels, and climate change (Tanir et al., 2024). This trend underscores the urgent need for improved HAB monitoring, estimation, modeling, and prediction techniques to safeguard water resources and public health (Greene et al., 2021; Ratté-Fortin et al., 2023; Paerl et al., 2016; Yan et al., 2024b).

Lake Erie, as part of the Great Lakes system, provides a compelling case study for investigating HABs. The Great Lakes represent the largest and most biodiverse freshwater system on Earth (Magnuson et al., 1997; Tewari et al., 2022). With both industrial and agricultural regions in its basin, Lake Erie is the shallowest and smallest of the Great Lakes by volume, yet it holds ecological, cultural, and economic importance for approximately 12.5 million residents within its watershed. Lake Erie supports commercial and traditional fisheries, extensive freight transport, and a robust recreation and tourism industry (Sterner et al., 2020). Its western basin is particularly prone to nutrient overload, primarily due to its geographical setting (Boegehold et al., 2023). Since 2002, chlorophyll-a (Chl-a) concentrations, a widely accepted indicator of eutrophication and HABs, have risen to unprecedented levels (Stumpf et al., 2016; Boegehold et al., 2023). Humans face exposure to HABs through ingestion, drinking water, and recreational activities (Carmichael and Boyer, 2016; Buratti et al., 2017). Therefore, predicting HAB occurrences is essential for minimizing health, economic, and environmental risks. Identifying the key factors driving these blooms is crucial for implementing effective mitigation strategies (Kouakou and Poder, 2019).

HAB formation typically results from the interplay of various factors that foster favorable growth conditions (Wells et al., 2015). Eutrophication, poor water quality—especially elevated nitrogen and phosphorus levels—and climate change are among the primary contributors (Glibert, 2020; Zhou et al., 2022). While past studies have examined individual drivers such as nutrients, land use, or climate, few have explored the complex interactions between physical, chemical, and biological factors (Wells et al., 2020; Maze et al., 2015; Paerl et al., 2011). Previous studies, such as Hushchyna et al. (2023), have highlighted key nutrient drivers like total phosphorus (TP) and iron in predicting cyanobacterial bloom intensity in Lake Torment, Nova Scotia, emphasizing the

broader significance of nutrient management in mitigating HABs across freshwater systems. These approaches often rely on limited data, which can oversimplify predictions and introduce potential inaccuracies. Therefore, understanding the multifaceted drivers of HABs is critical for effective monitoring and prevention.

Traditional HAB monitoring techniques, including laboratory analysis of chlorophyll-a, cyanobacteria, and various algal toxins, are labor-intensive and require specialized expertise (Katin et al., 2021; Giere et al., 2020; Greer et al., 2016). Remote sensing technologies, such as satellite and UAV data, offer valuable spatial insights into understanding environmental drivers (Li et al., 2023; Li and Demir, 2024) including bloom dynamics (Rolim et al., 2023; Kislik et al., 2022; Cheng et al., 2020). However, the relationship between chlorophyll-a levels and algal toxicity is complex, varying by location and environmental conditions (Hartshorn et al., 2016; Hollister and Kreakie, 2016). Furthermore, higher chlorophyll-a concentrations do not always signify high toxin levels but may indicate a higher probability of exceeding certain thresholds (Hollister and Kreakie, 2016). Therefore, understanding the main drivers of HABs remains pivotal for accurate prediction and prevention efforts.

Various prediction models have been developed to address HAB dynamics. Physical process-based models, such as the Environmental Fluid Dynamic Code (EFDC) (Zheng et al., 2021), QUAL2K (Bui et al., 2019) and Water Quality Analysis Simulation (WASP) (Wool et al., 2020), rely on detailed physical and biochemical processes but face challenges in handling spatial data and high costs (Shin et al., 2019; Verhamme et al., 2016; Wynne et al., 2013; Baek et al., 2021). While these models have high prediction accuracy with complete data, constructing perfect data, particularly with spatial resolution, is costly and involves practical limitations. Statistical models that correlate physicochemical and meteorological variables (Sit et al., 2021a) often struggle with capturing nonlinear relationships (Liu and Zhang, 2022; Baydaroğlu et al., 2024), limiting their predictive accuracy (Frank et al., 2018). Both approaches contribute valuable insights but face limitations in predicting HAB dynamics under varied conditions (Janssen et al., 2019).

To address these challenges, data-driven models have emerged as promising alternatives for predicting HABs. These models, increasingly applied in hydrology, water resources, and environmental management, can uncover complex relationships without the need for explicit mathematical modeling of unknown processes (Tounsi et al., 2023; Wang et al., 2019). Data-driven approaches (Sit et al., 2021b) offer a significant advantage in analyzing and predicting HAB occurrences, providing more accurate and reliable results and support informed decisions for public through visualization and communication systems (Demir et al., 2009; Demir and Beck, 2009).

The objective of this study is to quantitatively identify the key physical, chemical, and biological drivers of HABs using multivariate regression analysis. Specifically, we aim to (1) assess the relative importance of explanatory variables, (2) identify the major drivers of HAB dynamics, and (3) quantify the relationship between water quality variables and HAB formation. Statistical methods such as correlation analysis, multivariate regression analysis, and the ANOVA F-test were applied to our dataset. In addition, multivariate regression analysis was also conducted

for total suspended solids (TSS), which is an important indicator for monitoring water quality and measuring the degree of water pollution, to further demonstrate the robustness of our approach. The HAB analysis framework developed in this study is designed for broad application to lakes, rivers, and coastal areas. We anticipate that this framework will serve as a valuable tool for scientists and stakeholders, offering practical guidance for understanding and mitigating HAB risks globally. This paper is structured as follows: Section 2 describes the methodology, including data collection and correlation and multivariate regression analysis. Section 3 presents the results and discussion, highlighting the key drivers for HAB. Section 4 concludes with insights into the implications of the findings and suggestions for future research.

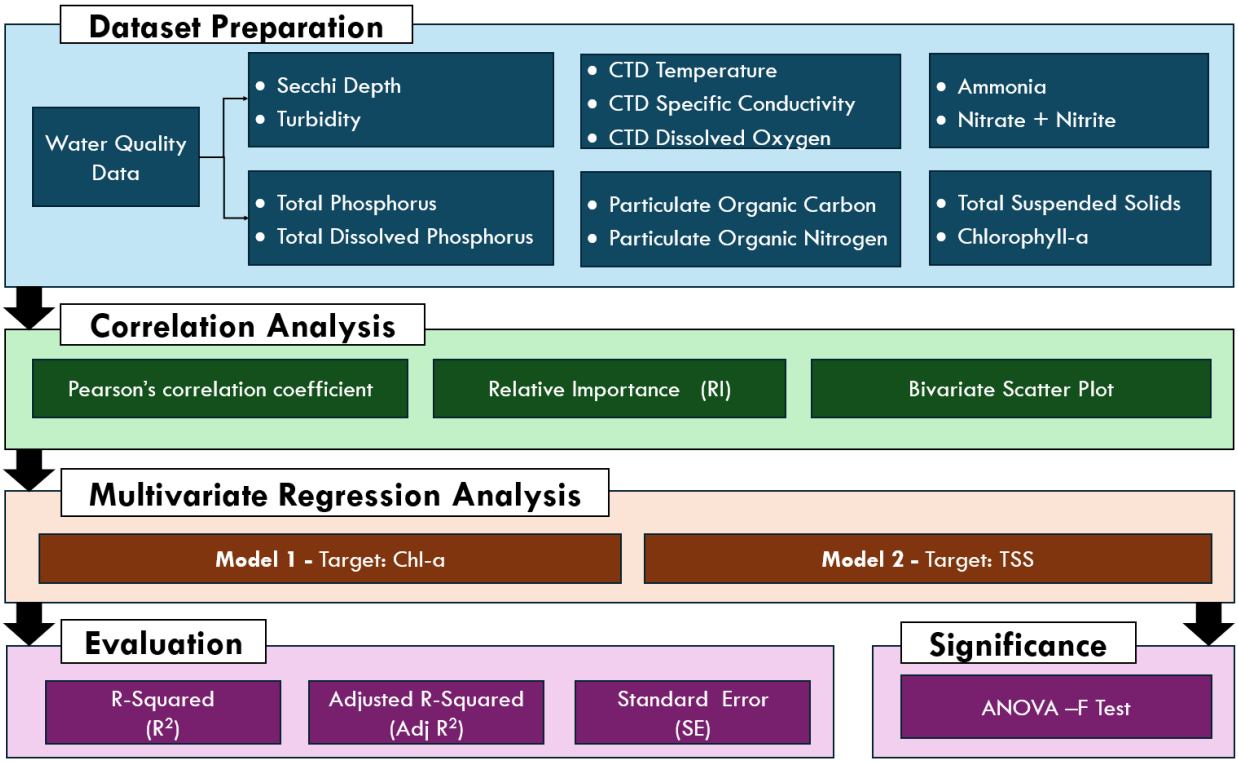

Figure 1. Workflow of the proposed study for analyzing the key drivers of HABs

2. Materials and Methods

Figure 1 outlines the workflow for the proposed study, starting with dataset preparation, where water quality data undergoes preprocessing to address missing values, remove duplicate records, and ensure data consistency. In the *Correlation Analysis* phase, the relationships between the water quality variables and the target variables (Chl-a and TSS) are examined using Pearson's correlation coefficient. Additionally, the Relative Importance (RI) index is employed to determine the influence of each predictor variable, while bivariate scatter plots visualize the linear relationships. This analysis identifies the key water quality parameters that exhibit statistically significant correlations with the target variables. The third stage involves *Multivariate Regression Analysis*, where two separate models are developed: Model 1, which focuses on predicting Chl-a

concentrations, and Model 2, which targets the prediction of TSS levels. These models aim to uncover the functional relationships between the predictors and the target variables, considering the complexity and interdependence of the environmental factors.

2.1. Data Collection and Pre-processing

As the nutrient load and HAB occurrence in Lake Erie take place mostly at the western part, our study was focused on the western basin of Lake Erie (shown in Figure 2), which encompasses the western part of the lake to Point Pelee, ON, Canada and Cedar Point, OH, USA. In this study, we used water quality data collected from multiple monitoring stations (Fig. 1) at the western part of Lake Erie on the US side operated by National Oceanic and Atmospheric Administration (NOAA) Great Lakes Environmental Research Laboratory (GLERL). The data were sampled from 2013 to 2020, and the resolution of data is in units of days (Boegehold et al., 2023). We specifically focused on monitoring stations closest to Maumee River inflow (i.e., WE06 and WE09) which reflect the various nutrient and sediment input into the western basin of Lake Erie as well as represent the area that are prone to HAB consistently compared to other stations further out in the western part of the lake (Stumpf et al., 2016).

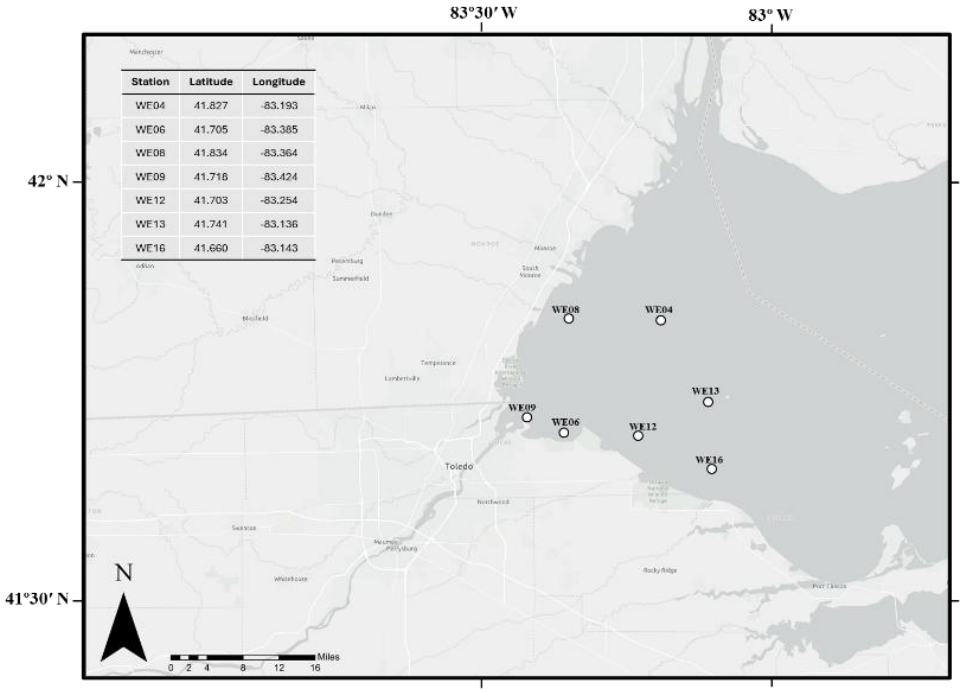

Figure 2. Location and description western Lake Erie water quality monitoring stations.

Based on the available data, we selected physical, chemical and biological variables, shown in Table 1. Physical variables include Secchi Depth, CTD Temperature, CTD Specific Conductivity, and Turbidity. Chemical drivers also include CTD Dissolved Oxygen, Total Phosphorus, Total Dissolved Phosphorus, Ammonia, Nitrate + Nitrite, Particulate Organic Carbon, Particulate

Organic Nitrogen, and Total Suspended Solids. Chlorophyll-a is also categorized under the biological variables.

Table 1. Summary of the variables used in this study

Variable	Abbr.	Unit	Definition
Secchi Depth	SD	m	Penetration depth of sunlight through the water
CTD Temperature	T	°C	Water temperature at site
CTD Specific Conductivity	Cond	µS/cm	Conductivity value of water at site
CTD Dissolved Oxygen	DO	mg/L	Concentration of dissolved oxygen at site
Turbidity	Turb	NTU	Cloudiness of a fluid caused by suspended solids
Total Phosphorus	TP	µg/L	Concentration of the sum of all phosphorus compounds that occur in various forms at site
Total Dissolved Phosphorus	TDP	µg /L	Concentration of the portion of phosphorus that is dissolved at site
Ammonia	A	µg /L	Concentration of Ammonia at site
Nitrate + Nitrite	N		Concentration of NO_x at site
Particulate Organic Carbon	POC	mg/L	Concentration of organic carbon particles suspended in water at site
Particulate Organic Nitrogen	PON	mg/L	Concentration of organic nitrogen particles suspended in water at site
Total Suspended Solids	TSS	mg/L	Concentration of both organic and inorganic particles suspended in water at site
Chlorophyll-a	Chl-a	µg /L	Indicator of HABs

2.2. Correlation Analysis

In this work, Pearson's correlation coefficient, which is the pivotal statistical techniques, was used to analyze the correlation between two variables. The Pearson correlation coefficient method is aimed at assessing linear variable correlations. The correlation coefficient is typically denoted by the symbol r, whose values range between -1 and 1, where 1 indicates strong positive correlation, -1 indicates strong negative correlation, and a value near 0 suggests a weak or nonexistent relationship (Gogtay and Thatte, 2017). r can be calculated using Eq. (1):

$$r = \frac{\sum_{i=1}^{n}(x_i - \bar{x})(y_i - \bar{y})^2}{\sum_{i=1}^{n}(x_i - \bar{x})^2 \sum_{i=1}^{n}(y_i - \bar{y})^2} \quad (1)$$

where r is the Pearson's correlation coefficient, N is the sample size, and x_i and y_i is the i^{th} sample values, $\bar{x}$ and $\bar{y}$ is the mean values of x and y. In addition, an absolute value of r more than 0.8 means a strong correlation, < 0.2 means a weak correlation, and between 0.2 and 0.8 indicates a correlation (Wang et al., 2023).

2.3. Multivariate Regression Analysis

Multivariate analysis is essential for categorizing environmental drivers (i.e. HABs) with similar traits and summarizing related multivariate patterns, offering valuable insights for creating targeted mitigation strategies (Xu et al., 2019a; 2019b). Multivariate regression analysis was performed to develop a regression model between the dependent variable and different independent variables. The Chl-a and TSS were set as the dependent variables for our study. To avoid the influence of collinearity on the regression analysis, independent variables were selected by comparing the relative importance values. A simple correlation analysis was performed to estimate the correlations between the dependent variable and independent variables. Then multivariate regression analysis was performed using the least squares method. When there are *n* independent variables (X_i), dependent variable (Y) can be described under the form of the below equation:

$$Y = b_0 + b_1X_1 + b_2X_2 + ... + b_nX_n + \epsilon \quad (2)$$

From Eq. (2), it can be seen that the regression coefficient, or slope, b_i (unbiased estimate), represents the change in Y per unit change in the (Xi) variable after the adjustment for simultaneous linear change; and the y-intercept, b_0, also called the multi-regression constant, standing for the y value where the regression line crosses the y-axis. Hence, it is the value of y when the value of x is equal to 0. The last parameter ϵ in Eq. (2) represents the residuals (error term). Eq. (2) can be very helpful in predicting the value of the dependent variable (Y) from the given value of the independent variables (X_i). It also may predict Y from the outer given ranges of (X_i), but such extrapolation is not highly recommended (Kelley & Bolin, 2013). We have also herein the ANOVA-F test in our regression model to nullify our hypothesis that there is no relationship between the independent variable (X) and dependent (Y) variable, i.e., all regression coefficients equal to zero ($b_1 = b_2 = ... = b_n = 0$). From the ANOVA-F test, the significant p-value (< 0.05 at 95% confidential interval) suggests that the relationship between (X_i) and Y is crucial. The independent variables (X_i) can reliably predict the dependent variable Y

2.4. Coefficients of Determination

Coefficients of Determination (R^2) indicates how well the predictive value explains the measured value. In this work, measured and predicted Chl-a (and TSS) concentrations were taken as the dependent and independent variables respectively, and the R^2 was determined by applying linear regression analysis. The R^2 ranges from 0 to 1; the closer the value is to 1, the better the independent variable explains the dependent variable, meaning the higher the prediction accuracy. The formula for R^2 is as follows:

$$R^2 = 1 - \frac{\sum_{i=1}^{n}(y_i - \hat{y}_i)^2}{\sum_{i=1}^{n}(y_i - \bar{y})^2} \quad (3)$$

where y_i is the i^{th} actual value and $\hat{y}$ is the i^{th} predicted value of the dependent variable, and $\bar{y}$ is the mean of y_i. The adjusted R^2, which is defined as corrected value of R^2 for sample size and regression coefficients, is a better parameter than R^2 itself. The adjusted R^2 is always less than R^2. A high or adjusted R^2 generally represents the better model but is not always correct and should be used with caution to asset the model. There is no cutoff point of R^2 for the appropriate model selection. R^2 should be evaluated based on the field data types, data transformations, or subject area decisions (Hair et al., 2010).

3. Results and Discussions

Table 2 shows a summary of the descriptive statistics of the dataset after pre-processing. In the table, Particulate Organic Carbon and Particulate Organic Nitrogen levels varied widely as well, with maximums far exceeding the average, suggesting the presence of organic matter in different concentrations throughout the samples. On the other hand, Total Suspended Solids and Chlorophyll-a also showed large ranges in value, pointing to varied conditions in the sampled water bodies. The standard deviation for each variable suggests the extent of variation in the measurements, with some variables like turbidity and total phosphorus showing very high variability. It is noticed that we have in total 13 parameters, and we distinguish these parameters into two different targets, including Chl-a and TSS versus predictors (the rest of the parameters).

Table 2. Statistical description of the dataset used in this study

Variables	Min	Max	Mean	Std. Dev.
SD	0	5.3	0.796	0.694
T	10.1	29.7	22.417	3.651
Cond	19.9	583.3	337.586	67.828
DO	4.2	13.0	7.478	1.217
Turb	0.95	1148.0	29.599	78.295
TP	14.87	2482.2	119.144	181.173
TDP	2.67	273.6	30.909	34.865
A	0.04	561.6	39.822	56.930
N	0	9.5	1.308	1.676
POC	0.15	219.3	3.946	15.381
PON	0.03	40.9	0.677	2.759
TSS	1.25	540.8	25.489	44.275
Chl-a	0.71	6784.0	61.232	347.307

Table 3 presents the Relative Importance (RI) values for each predictor variable in relation to Chlorophyll-a (Chl-a) and Total Suspended Solids (TSS). For Chl-a, Particulate Organic Nitrogen (PON), Turbidity, and Particulate Organic Carbon (POC) emerge as the most influential variables, contributing 24.26%, 22.77%, and 18.39% to the model, respectively. These factors play a critical

role in explaining the variability of Chl-a concentrations in the water. Other significant contributors include Total Suspended Solids (TSS) and Total Phosphorus (TP), accounting for 13.00% and 10.01%, respectively. However, the remaining variables, such as Secchi Depth (SD), Dissolved Oxygen (DO), and Temperature (T), provide minimal contributions, and variables like Conductivity (Cond) and Nitrogen (N) contribute even less.

For the TSS model, Turbidity (35.57%), PON (28.06%), and POC (24.12%) dominate the model, collectively explaining most of the variance in TSS. Chl-a itself accounts for 5.34% of the variance, while TP (6.20%) also plays a notable but smaller role. The remaining variables, including SD, TDP, T, and others, contribute very little, with some variables, such as DO and Cond, having no measurable importance. This analysis emphasizes the crucial role of certain particulate components (PON, Turb, and POC) in both models, highlighting them as key drivers in understanding the dynamics of both Chl-a and TSS in the context of harmful algal blooms in Lake Erie.

Table 3. Relative Importance (RI) value for two considered targets

	RI for Chl-a (100%)	**RI for TSS (100%)**
PON	24.26	28.06
Turb	22.77	35.57
POC	18.39	24.12
TSS	13.00	---
TP	10.01	6.20
SD	3.14	0.34
DO	2.44	0.00
T	2.19	0.15
TDP	2.01	0.12
A	1.25	0.11
Cond	0.50	0.00
N	0.05	0.01
Chl-a	---	5.34

Table 4 presents the Pearson correlation coefficients between all target variables and regressors. Pearson correlation coefficients indicate the strength and direction of the linear relationship between two variables, ranging from -1 (perfect negative correlation) to 1 (perfect positive correlation). A value close to 0 suggests no correlation. This correlation matrix provides important insights into the relationships between environmental variables and the two target variables, Chl-a and TSS. The strongest drivers for Chl-a are PON, Turbidity, and POC, while TSS is primarily influenced by Turbidity, PON, and POC.

Figure 3 also shows a bivariate scatter plot indicating pairwise relationships between seven selected regressors, SD, Turb, TP, POC, PON, TSS, and Chl-a, for this analysis. Clear positive linear relationships are observed between Turbidity and TSS, as well as between Turbidity, POC,

PON, and Chl-a, suggesting that these variables are important drivers of both suspended solids and algal bloom concentration. TP also shows moderate positive associations with both turbidity and Chl-a, reinforcing the role of phosphorus in contributing to water turbidity and algal growth.

Table 4. Pearson's correlation coefficients for all target variables and regressors

	SD	T	Cond	DO	Turb	TP	TDP	A	N	POC	PON	TSS	Chl-a
SD	1.00	0.12	-0.13	-0.05	-0.23	-0.27	-0.15	-0.06	-0.01	-0.12	-0.11	-0.35	-0.06
T	0.12	1.00	-0.01	-0.32	-0.07	-0.06	-0.06	-0.15	0.06	0.06	0.06	-0.16	0.07
Cond	-0.13	-0.01	1.00	-0.15	-0.04	0.09	0.40	0.39	0.50	-0.06	-0.06	-0.03	-0.05
DO	-0.05	-0.32	-0.15	1.00	0.10	0.03	-0.31	-0.32	-0.23	0.16	0.16	0.06	0.19
Turb	-0.23	-0.07	-0.04	0.10	1.00	0.88	0.11	0.06	0.05	0.89	0.91	0.93	0.75
TP	-0.27	-0.06	0.09	0.03	0.88	1.00	0.28	0.14	0.19	0.76	0.78	0.83	0.69
TDP	-0.15	-0.06	0.40	-0.31	0.11	0.28	1.00	0.48	0.61	-0.08	-0.08	0.17	-0.06
A	-0.06	-0.15	0.39	-0.32	0.06	0.14	0.48	1.00	0.46	-0.09	-0.09	0.12	-0.08
N	-0.01	0.06	0.50	-0.23	0.05	0.19	0.61	0.46	1.00	-0.09	-0.08	0.09	-0.07
POC	-0.12	0.06	-0.06	0.16	0.89	0.76	-0.08	-0.09	-0.09	1.00	0.99	0.78	0.71
PON	-0.11	0.06	-0.06	0.16	0.91	0.78	-0.08	-0.09	-0.08	0.99	1.00	0.76	0.79
TSS	-0.35	-0.16	-0.03	0.06	0.93	0.83	0.17	0.12	0.09	0.78	0.76	1.00	0.49
Chl-a	-0.06	0.07	-0.05	0.19	0.75	0.69	-0.06	-0.08	-0.07	0.71	0.79	0.49	1.00

In this study, the objective is to deal with multivariate regression showing the association between dependent and independent variables. With our data after evaluating the relative importance and correlation analysis, two regression models have been determined as below for the prediction Chl-a and TSS, including:

Model 1: Chl-a= 0.113 Tur - 0.035 TP - 3.453 POC + 4.115 PON - 0.03 TSS + 0.004 (4)

Model 2: TSS= 1.477 Tur + 0.196 TP + 2.125 POC - 2.705 PON -0.126 Chl-a + 0.007 (5)

In Table 5, multivariate correlation coefficient (r) provides insight into the strength and direction of the relationship between independent and dependent variables in our regression models. For Model 1, the r-value is 0.986, indicating a very strong positive correlation, which suggests a high-quality prediction for the dependent variable, Chl-a. Similarly, in Model 2, the r-value is 0.979, also signifying a strong predictive relationship, this time for the dependent variable TSS. The coefficients of determination, represented by R^2 and adjusted R^2, further emphasize the model's effectiveness in explaining the variability in the outcome variable. In Model 1, R^2 is 0.973, meaning 97.3% of the variance in Chl-a can be attributed to the independent variables in the regression model. The adjusted R^2, which accounts for the number of predictors in the model, remains at 0.973, confirming that the predictors explain the vast majority of variability without overfitting.

Model 2 follows a similar trend, with R^2 at 0.958, indicating that 95.8% of the variability in TSS is explained by the independent variables. The adjusted R^2 for Model 2 also mirrors this value, reflecting the robustness of the model. The standard error (SE) of the estimate provides a measure

of the average distance that the observed values fall from the regression line. For Model 1, the SE is 0.008, indicating a very small error in the predictions of Chl-a. In Model 2, the SE is slightly higher at 0.016, which still reflects a reasonably accurate prediction for TSS. In both models, the low SE values reinforce the precision and reliability of the regression models, indicating minimal deviation between the observed and predicted values.

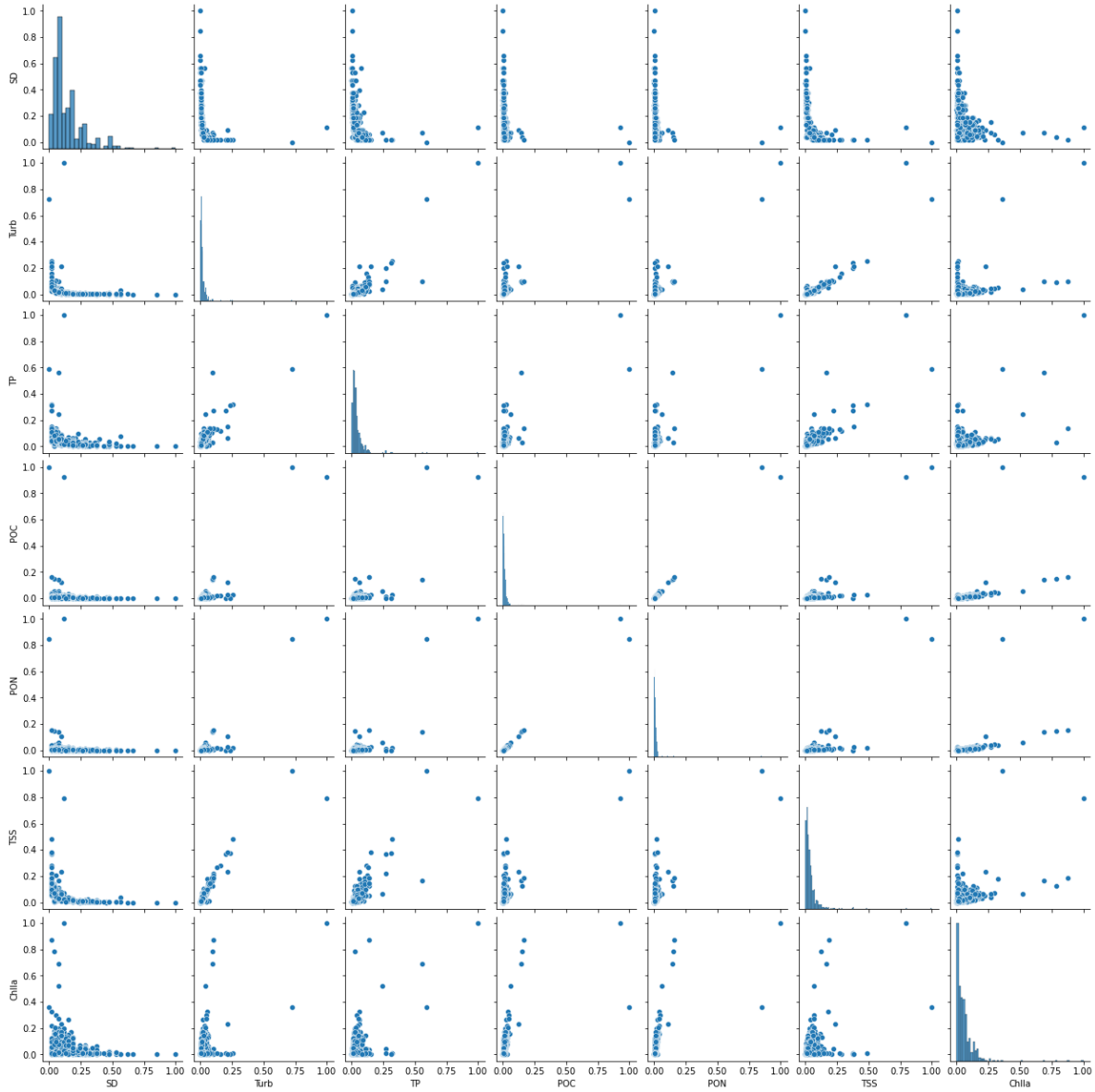

Figure 3. Bivariate scatter plots for seven selected regressors.

Table 5. Model summary

	r	R^2	Adjusted R^2	Std. Error (SE)
Model 1	0.986	0.973	0.972	0.008
Model 2	0.979	0.958	0.957	0.016

In Table 6, the ANOVA table provides crucial information regarding the statistical significance of our regression models. The table presents two primary components: the regression and residual sum of squares, which are used to evaluate how well the independent variables explain the variance in the dependent variable. In Model 1, which predicts Chl-a, the F-ratio of 3250.46 is substantially larger than 1, indicating a highly significant regression model. The F-ratio represents the ratio of the mean square for the regression to the mean square for the residuals, which compares the variance explained by the model to the variance that remains unexplained. A high F-ratio suggests that the model explains a considerable amount of variation in the dependent variable. The associated p-value is reported as less than $1E^{-4}$, confirming that this result is statistically significant and that the likelihood of these findings occurring by chance is extremely low.

Therefore, we can conclude that the independent variables used in Model 1 are strong predictors of Chl-a, and the model is a good fit for the data. Similarly, for Model 2, which predicts TSS, the F-ratio is 2067.33, again significantly larger than 1. This high F-value suggests that the independent variables in this model also explain a substantial amount of the variability in TSS. The p-value for this model is also less than $1E^{-4}$, reinforcing the statistical significance of the model. This indicates that the relationship between the independent variables and TSS is robust, and the model fits the data well. Overall, the results presented in Table 6 demonstrate that both regression models are statistically significant, meaning that the independent variables are highly effective in predicting the respective dependent variables, Chl-a and TSS.

Table 6. ANOVA table for statistical significance

		df	SS - Sum of Square	MS - Mean Squares	F-ratio	p-value
Model 1						
	Regression	5	0.989	1.98E-01	3250.46	< 1E-4
	Residual	453	0.028	6.09E-05		
	Total	458	1.017			
Model 2						
	Regression	5	2.598	5.20E-01	2067.33	< 1E-4
	Residual	453	0.114	2.51E-04		
	Total	458	2.712			

Table 7 presents the estimated coefficients for the multivariate regression models predicting Chl-a in Model 1 and TSS in Model 2. These unstandardized coefficients represent the direct impact of each independent variable on the dependent variable, holding all other predictors constant. Each coefficient in the regression equation explains how much the dependent variable is expected to increase or decrease with a one-unit change in the independent variable. For Model 1, the regression equation is:

$$\text{Chl-a} = 0.113\times\text{Turb} - 0.035\times\text{TP} - 3.453\times\text{POC} + 4.115\times\text{PON} - 0.03\times\text{TSS} + 0.004.$$

This equation allows for the prediction of Chl-a based on the values of five independent variables: Turb, TP, POC, PON, and TSS. For Model 2, the regression equation is:

$$TSS=1.477\times Turb+0.196\times TP+2.125\times POC-2.705\times PON-0.126\times Chl\text{-}a+0.007.$$

This equation will help to predict the TSS from the given value of three independent variables (Turb, TP, POC, PON, and Chl-a). The p-values associated with each variable provide insight into the statistical significance of these coefficients. P- values shown in Table 6 are different from 0 and most of them are less than 0.05 (except TSS for model 1 and Chl-a for model 2), indicating that these variables have a meaningful effect on target variables. The standard error (SE) values in the table measure the variability of the coefficients. Smaller SE values indicate that the estimates are more precise. In Model 1, all independent variables have small SEs, suggesting stable estimates. In Model 2, although most parameters have small SEs, POC and PON have slightly larger SEs, indicating more variability in their estimates.

Table 7. Estimates of coefficients for multivariate regression models

	Unstandardized Coefficients	**Standard Error (SE)**	**t**	**p-value**
Model 1				
Constant	0.004	0.000	7.906	< 0.0001
Turb	0.113	0.038	2.963	0.0032
TP	-0.035	0.012	-2.837	0.0048
POC	-3.453	0.076	-45.688	< 0.0001
PON	4.115	0.091	45.380	< 0.0001
TSS	-0.030	0.023	-1.319	0.1879
Model 2				
Constant	0.007	0.001	6.583	< 0.0001
Turb	1.477	0.037	40.445	< 0.0001
TP	0.196	0.023	8.392	< 0.0001
POC	2.125	0.350	6.077	< 0.0001
PON	-2.705	0.415	-6.521	< 0.0001
Chl-a	-0.126	0.095	-1.319	0.1879

The correlation analysis reveals that PON, turbidity, and POC exhibit the strongest associations with Chl-a and TSS, suggesting these variables play crucial roles in algal bloom formation. Only relative importance value RI >5% can be considered (see Table 3). Specifically, PON and POC were found to have the highest relative importance values in the model, contributing over 20% each to the predictive capacity for Chl-a. These findings support the emphasis on nutrient management, as controlling organic nitrogen levels can mitigate bloom intensity and frequency,

potentially due to its role in nutrient cycling and algal growth (Wang et al., 2011; Du et al., 2022; Hushchyna et al.,2023).

Two linear multivariate regression models were suggested to predict Chl-a and TSS. Model 1 and Model 2 demonstrate robust predictive performance, with R^2 values of 0.973 for Chl-a and 0.958 for TSS respectively, indicating that our selected variables explain a significant proportion of the variance in HAB dynamics. The ANOVA F-test results further affirm model significance ($F = 3250.46$ for Chl-a; $F = 2067.33$ for TSS), underscoring the reliability of our predictors. For both models, all the variables are statistically significant to the prediction (p-value < 0.05). These two models with statistically significant analyses show that the prediction for Chl-a and TSS could be well performed for Lake Erie.

It can be seen in Table 7, for model 1 all parameters except TSS are significant (p-value < 0.05), and we can infer that there is an association between all variables. For model 2, Turb, TP, POC, and PON are significant as p-value <0.05, while Chl-a is insignificant as the p-value is greater than 0.05, saying that there is more association between the variables than Chl-a. High levels of TP contribute positively to Chlorophyll-a concentrations, highlighting its importance as a nutrient that supports algal growth. This aligns with ecological understanding, as phosphorus is a key nutrient that often limits primary productivity in aquatic systems (Havens et al., 2003; Zhang et al., 2024; Demiray et al., 2024).

Our analysis underscores the importance of managing specific nutrients, particularly phosphorus and nitrogen compounds, to reduce HAB risk in Lake Erie. The high predictive accuracy achieved by including TP, PON, turbidity, and POC as independent variables suggests that nutrient reduction strategies targeting these factors could effectively mitigate algal blooms. This aligns with findings from several literatures, suggesting that nutrient load control is a universally applicable management approach for HABs across diverse freshwater ecosystems (Hushchyna et al.,2023; Rosales et al., 2022).

4. Conclusions

This study presents a detailed analysis of the environmental drivers influencing Harmful Algal Blooms (HABs) in Lake Erie, using a multivariate regression approach to develop predictive models for chlorophyll-a (Chl-a) and total suspended solids (TSS). Through the integration of physical, chemical, and biological variables collected from multiple monitoring stations over seven years, our models identified particulate organic nitrogen (PON), turbidity, and particulate organic carbon (POC) as the most critical predictors of HAB dynamics. The statistical models demonstrated a strong fit, with R^2 values of 0.973 for Chl-a and 0.958 for TSS, underscoring the robustness of multivariate regression for capturing the complex interactions between water quality variables and HAB occurrences.

The significance of this research lies in its ability to uncover key environmental factors that drive HAB formation, offering valuable insights into water quality management in Lake Erie and beyond. The study's framework can be broadly applied to other aquatic ecosystems, where similar environmental pressures contribute to harmful algal growth. By improving our understanding of

these drivers, the study enables more accurate and proactive HAB forecasting, which is critical for safeguarding public health, protecting aquatic ecosystems, and mitigating economic losses in sectors such as fisheries, tourism, and water supply management.

Moreover, this study emphasizes the importance of using comprehensive datasets and advanced statistical methods to explore the multifaceted relationships between water quality variables. While the models used in this study demonstrate strong predictive capacity, future research should investigate the integration of real-time monitoring systems and machine learning techniques to enhance the adaptability and accuracy of HAB prediction models under varying environmental conditions. Additionally, exploring non-linear modeling approaches could provide further insights into the threshold effects and tipping points that lead to bloom occurrences.

In conclusion, this research represents an important step toward developing data-driven tools for HAB management. By identifying the key drivers of HABs and constructing accurate prediction models, this study contributes to the development of evidence-based management strategies that can mitigate the risks posed by HABs. Policymakers, environmental agencies, and stakeholders can leverage these findings to implement targeted interventions, such as nutrient load reductions and enhanced monitoring efforts, ultimately fostering a more sustainable and resilient approach to managing freshwater resources.

5. References

Baek, S. S., Kwon, Y. S., Pyo, J., Choi, J., Kim, Y. O., & Cho, K. H. (2021). Identification of influencing factors of A. catenella bloom using machine learning and numerical simulation. Harmful Algae, 103, 102007.

Bayar, S., Demir, I., & Engin, G. O. (2009). Modeling leaching behavior of solidified wastes using back-propagation neural networks. Ecotoxicology and environmental safety, 72(3), 843-850.

Baydaroğlu, Ö. (2025). Harmful algal bloom prediction using empirical dynamic modeling. Science of The Total Environment, 959, 178185.

Baydaroğlu, Ö., Yeşilköy, S., Dave, A., Linderman, M., Demir, I. (2024). Modeling of Harmful Algal Bloom Dynamics and the Model-Based Interactive Framework for Inland Waters. EarthArxiv, 7075. https://doi.org/10.31223/X5S40X.

Boegehold, A. G., Burtner, A. M., Camilleri, A. C., Carter, G., DenUyl, P., Fanslow, D., Fyffe Semenyuk, D., Godwin, C. M., Gossiaux, D., Johengen, T. H., Kelchner, H., Kitchens, C., Mason, L. A., McCabe, K., Palladino, D., Stuart, D., Vanderploeg, H., and Errera, R. (2023). Routine monitoring of western Lake Erie to track water quality changes associated with cyanobacterial harmful algal blooms. Earth System Science Data Discussions, 2023, 1-39.

Bui, H. H., Ha, N. H., Nguyen, T. N. D., Nguyen, A. T., Pham, T. T. H., Kandasamy, J., & Nguyen, T. V. (2019). Integration of SWAT and QUAL2K for water quality modeling in a data scarce basin of Cau River basin in Vietnam. Ecohydrology & Hydrobiology, 19(2), 210-223.

Buratti, F. M., Manganelli, M., Vichi, S., Stefanelli, M., Scardala, S., Testai, E., and Funari, E. (2017). Cyanotoxins: producing organisms, occurrence, toxicity, mechanism of action and human health toxicological risk evaluation, Arch. Toxicol., 91, 1049-1130.

Carmichael, W. W. and Boyer, G. L. (2016). Health impacts from cyanobacteria harmful algae blooms: Implications for the North American Great Lakes, Harmful Algae, 54, 194-212.

Carmichael, W. W., & Falconer, I. R. (1993). Diseases related to freshwater blue-green algal toxins, and control measures. In I.R. Falconer (Ed.). Algal toxins in seafood and drinking water (pp.187-209). London: Academic Press

Cheng, K. H., Chan, S. N., & Lee, J. H. (2020). Remote sensing of coastal algal blooms using unmanned aerial vehicles (UAVs). Marine Pollution Bulletin, 152, 110889.

Demir, I., & Beck, M. B. (2009, April). GWIS: a prototype information system for Georgia watersheds. In Georgia Water Resources Conference: Regional Water Management Opportunities, UGA, Athens, GA, US.

Demir, I., Jiang, F., Walker, R. V., Parker, A. K., & Beck, M. B. (2009, October). Information systems and social legitimacy scientific visualization of water quality. In 2009 IEEE International Conference on Systems, Man and Cybernetics (pp. 1067-1072). IEEE.

Demiray, B. Z., Mermer, O., Baydaroğlu, Ö., & Demir, I. (2025). Predicting harmful algal blooms using explainable deep learning models: a comparative study. Water, 17(5), 676.

Du, Y., An, S., He, H., Wen, S., Xing, P., & Duan, H. (2022). Production and transformation of organic matter driven by algal blooms in a shallow lake: Role of sediments. Water Research, 219, 118560.

Franks, P. J. (2018). Recent advances in modelling of harmful algal blooms. Global ecology and oceanography of harmful algal blooms, 359-377.

Giere, J., Riley, D., Nowling, R. J., McComack, J., & Sander, H. (2020). An investigation on machine-learning models for the prediction of cyanobacteria growth. Fundamental and Applied Limnology, 194(2), 85-94.

Glibert, P. M. (2020). Harmful algae at the complex nexus of eutrophication and climate change. Harmful algae, 91, 101583.

Graham, J. L., Dubrovsky, N. M., & Eberts, S. M. (2016). Cyanobacterial harmful algal blooms and US Geological Survey science capabilities. US Department of the Interior, US Geological Survey.

Greene, S. B. D., LeFevre, G. H., & Markfort, C. D. (2021). Improving the spatial and temporal monitoring of cyanotoxins in Iowa lakes using a multiscale and multi-modal monitoring approach. Science of the Total Environment, 760, 143327.

Greer, B., McNamee, S. E., Boots, B., Cimarelli, L., Guillebault, D., Helmi, K., ... & Campbell, K. (2016). A validated UPLC–MS/MS method for the surveillance of ten aquatic biotoxins in European brackish and freshwater systems. Harmful algae, 55, 31-40.

Hair, J. F, Anderson, R. E, Babin, B. J, & Black, W. C. (2010). Multivariate data analysis: A Global Perspective. 7th ed. Upper Saddle River (N.J.): Pearson education.

Hartshorn, N., Marimon, Z., Xuan, Z., Cormier, J., Chang, N. B., & Wanielista, M. (2016). Complex interactions among nutrients, chlorophyll-a, and microcystins in three stormwater wet detention basins with floating treatment wetlands. Chemosphere, 144, 408-419.

Havens, K. E. (2003). Phosphorus–algal bloom relationships in large lakes of south Florida: implications for establishing nutrient criteria. Lake and Reservoir Management, 19(3), 222-228.

Hollister, J. W., & Kreakie, B. J. (2016). Associations between chlorophyll-a and various microcystin health advisory concentrations. F1000Research, 5.

Hushchyna, K., Sabir, Q. U. A., Mclellan, K., & Nguyen-Quang, T. (2023). Multicollinearity and Multi-regression Analysis for Main Drivers of Cyanobacterial Harmful Algal Bloom (CHAB) in the Lake Torment, Nova Scotia, Canada. Environmental Modeling & Assessment, 28(6), 1011-1022.

Islam, S. S., Yeşilköy, S., Baydaroğlu, Ö., Yıldırım, E., & Demir, I. (2024). State-level multidimensional agricultural drought susceptibility and risk assessment for agriculturally prominent areas. International Journal of River Basin Management, 1-18.

Janssen, A. B., Janse, J. H., Beusen, A. H., Chang, M., Harrison, J. A., Huttunen, I., ... & Mooij, W. M. (2019). How to model algal blooms in any lake on earth. Current opinion in environmental sustainability, 36, 1-10.

Katin, A., Del Giudice, D., Hall, N. S., Paerl, H. W., & Obenour, D. R. (2021). Simulating algal dynamics within a Bayesian framework to evaluate controls on estuary productivity. Ecological Modelling, 447, 109497.

Kelley, K., & Bolin, J. H. (2013). Multiple regression. In Handbook of quantitative methods for educational research (pp. 69-101). Brill.

Kislik, C., Dronova, I., Grantham, T. E., & Kelly, M. (2022). Mapping algal bloom dynamics in small reservoirs using Sentinel-2 imagery in Google Earth Engine. Ecological Indicators, 140, 109041.

Kouakou, C. R., & Poder, T. G. (2019). Economic impact of harmful algal blooms on human health: a systematic review. Journal of water and health, 17(4), 499-516.

Li, Z., Xiang, Z., Demiray, B. Z., Sit, M., & Demir, I. (2023). MA-SARNet: A one-shot nowcasting framework for SAR image prediction with physical driving forces. ISPRS journal of photogrammetry and remote sensing, 205, 176-190.

Li, Z., & Demir, I. (2024). Better localized predictions with Out-of-Scope information and Explainable AI: One-Shot SAR backscatter nowcast framework with data from neighboring region. ISPRS Journal of Photogrammetry and Remote Sensing, 207, 92-103.

Liu, S. T., & Zhang, L. (2022). Surface Chaotic Theory and the Growth of Harmful Algal Bloom. In Surface Chaos and Its Applications (pp. 299-320). Singapore: Springer Nature Singapore.

Magnuson, J. J., Webster, K. E., Assel, R. A., Bowser, C. J., Dillon, P. J., Eaton, J. G., ... & Quinn, F. H. (1997). Potential effects of climate changes on aquatic systems: Laurentian Great Lakes and Precambrian Shield Region. Hydrological processes, 11(8), 825-871.

Maze, G., Olascoaga, M. J., & Brand, L. (2015). Historical analysis of environmental conditions during Florida Red Tide. Harmful Algae, 50, 1-7.

Paerl, H. W., Hall, N. S., & Calandrino, E. S. (2011). Controlling harmful cyanobacterial blooms in a world experiencing anthropogenic and climatic-induced change. Science of the total environment, 409(10), 1739-1745.

Paerl, H. W., & Paul, V. J. (2012). Climate change: links to global expansion of harmful cyanobacteria. Water research, 46(5), 1349-1363.

Paerl, H. W., Gardner, W. S., Havens, K. E., Joyner, A. R., McCarthy, M. J., Newell, S. E., ... & Scott, J. T. (2016). Mitigating cyanobacterial harmful algal blooms in aquatic ecosystems impacted by climate change and anthropogenic nutrients. Harmful Algae, 54, 213-222.

Ratté-Fortin, C., Plante, J. F., Rousseau, A. N., & Chokmani, K. (2023). Parametric versus nonparametric machine learning modelling for conditional density estimation of natural events: Application to harmful algal blooms. Ecological Modelling, 482, 110415.

Rolim, S. B. A., Veettil, B. K., Vieiro, A. P., Kessler, A. B., & Gonzatti, C. (2023). Remote sensing for mapping algal blooms in freshwater lakes: A review. Environmental Science and Pollution Research, 30(8), 19602-19616.

Rosales, D., Ellett, A., Jacobs, J., Ozbay, G., Parveen, S., & Pitula, J. (2022). Investigating the Relationship between nitrate, total dissolved nitrogen, and phosphate with abundance of pathogenic Vibrios and harmful algal blooms in Rehoboth Bay, Delaware. Applied and Environmental Microbiology, 88(14), e00356-22.

Shin, C. M., Kim, D., & Song, Y. (2019). Analysis of hydraulic characteristics of Yeongsan River and estuary using EFDC model. Journal of Korean Society on Water Environment, 35(6), 580-588.

Sit, M., Demiray, B., & Demir, I. (2021a). Short-term hourly streamflow prediction with graph convolutional gru networks. arXiv preprint arXiv:2107.07039.

Sit, M., Langel, R. J., Thompson, D., Cwiertny, D. M., & Demir, I. (2021b). Web-based data analytics framework for well forecasting and groundwater quality. Science of the Total Environment, 761, 144121.

Sterner, R. W., Keeler, B., Polasky, S., Poudel, R., Rhude, K., and Rogers, M. (2020). Ecosystem services of Earth's largest freshwater lakes, Ecosyst. Serv., 41, 101046.

Stumpf, R. P., Johnson, L. T., Wynne, T. T., & Baker, D. B. (2016). Forecasting annual cyanobacterial bloom biomass to inform management decisions in Lake Erie. Journal of Great Lakes Research, 42(6), 1174-1183.

Tanir, T., Yildirim, E., Ferreira, C. M., & Demir, I. (2024). Social vulnerability and climate risk assessment for agricultural communities in the United States. Science of The Total Environment, 908, 168346.

Tewari, M., Kishtawal, C. M., Moriarty, V. W., Ray, P., Singh, T., Zhang, L., ... & Tewari, K. (2022). Improved seasonal prediction of harmful algal blooms in Lake Erie using large-scale climate indices. Communications Earth & Environment, 3(1), 195.

Tounsi, A., Abdelkader, M., & Temimi, M. (2023). Assessing the simulation of streamflow with the LSTM model across the continental United States using the MOPEX dataset. Neural Computing and Applications, 35(30), 22469-22486.

Verhamme, E. M., Redder, T. M., Schlea, D. A., Grush, J., Bratton, J. F., & DePinto, J. V. (2016). Development of the Western Lake Erie Ecosystem Model (WLEEM): Application to connect phosphorus loads to cyanobacteria biomass. Journal of Great Lakes Research, 42(6), 1193-1205.

Wang, G., Zhou, W., Cao, W., Yin, J., Yang, Y., Sun, Z., ... & Zhao, J. (2011). Variation of particulate organic carbon and its relationship with bio-optical properties during a phytoplankton bloom in the Pearl River estuary. Marine pollution bulletin, 62(9), 1939-1947.

Wang, H., Zentar, R., & Wang, D. (2023). Predicting the compaction parameters of solidified dredged fine sediments with statistical approach. Marine Georesources & Geotechnology, 41(2), 195-210.

Wang, P., Yao, J., Wang, G., Hao, F., Shrestha, S., Xue, B., ... & Peng, Y. (2019). Exploring the application of artificial intelligence technology for identification of water pollution characteristics and tracing the source of water quality pollutants. Science of the Total Environment, 693, 133440.

Weirich, C. A., & Miller, T. R. (2014). Freshwater harmful algal blooms: toxins and children's health. Current problems in pediatric and adolescent health care, 44(1), 2-24.

Wells, M. L., Trainer, V. L., Smayda, T. J., Karlson, B. S., Trick, C. G., Kudela, R. M., ... & Cochlan, W. P. (2015). Harmful algal blooms and climate change: Learning from the past and present to forecast the future. Harmful algae, 49, 68-93.

Wells, M. L., Karlson, B., Wulff, A., Kudela, R., Trick, C., Asnaghi, V., ... & Trainer, V. L. (2020). Future HAB science: Directions and challenges in a changing climate. Harmful algae, 91, 101632.

Wool, T., Ambrose Jr, R. B., Martin, J. L., & Comer, A. (2020). WASP 8: The next generation in the 50-year evolution of USEPA's water quality model. Water, 12(5), 1398.

Wynne, T. T., Stumpf, R. P., Tomlinson, M. C., Fahnenstiel, G. L., Dyble, J., Schwab, D. J., & Joshi, S. J. (2013). Evolution of a cyanobacterial bloom forecast system in western Lake Erie: Development and initial evaluation. Journal of Great Lakes Research, 39, 90-99.

Xu, H., Muste, M., & Demir, I. (2019a). Web-based geospatial platform for the analysis and forecasting of sedimentation at culverts. Journal of Hydroinformatics, 21(6), 1064-1081.

Xu, H., Demir, I., Koylu, C., & Muste, M. (2019b). A web-based geovisual analytics platform for identifying potential contributors to culvert sedimentation. Science of the Total Environment, 692, 806-817.

Yan, Z., Kamanmalek, S., Alamdari, N., & Nikoo, M. R. (2024). Comprehensive Insights into Harmful Algal Blooms: A Review of Chemical, Physical, Biological, and Climatological Influencers with Predictive Modeling Approaches. Journal of Environmental Engineering, 150(4), 03124002.

Yeşilköy, S., & Demir, I. (2024). Crop yield prediction based on reanalysis and crop phenology data in the agroclimatic zones. Theoretical and Applied Climatology, 1-14.

Zhang, X., Li, Y., Zhao, J., Wang, Y., Liu, H., & Liu, Q. (2024). Temporal dynamics of the Chlorophyll a-Total phosphorus relationship and algal production efficiency: Drivers and management implications. Ecological Indicators, 158, 111339.

Zheng, L., Wang, H., Liu, C., Zhang, S., Ding, A., Xie, E., ... & Wang, S. (2021). Prediction of harmful algal blooms in large water bodies using the combined EFDC and LSTM models. Journal of Environmental Management, 295, 113060.

Zhou, Z. X., Yu, R. C., & Zhou, M. J. (2022). Evolution of harmful algal blooms in the East China Sea under eutrophication and warming scenarios. Water Research, 221, 118807.